Modelling cohesive crack growth using a two-step finite element-scaled boundary finite element coupled method

Z. J. Yang
Department of Engineering, University of Liverpool, Liverpool L69 3GH, UK

A. J. Deeks
School of Civil and Resource Engineering, the University of Western Australia, WA6009, Australia

ABSTRACT: This study develops a two-step method, coupling the finite element method (FEM) and the scaled boundary finite element method (SBFEM), to model cohesive crack growth in quasi-brittle normal-sized structures. In the first step, the crack trajectory is fully-automatically predicted by a remeshing procedure using the SBFEM based on linear elastic fracture mechanics theories. In the second, interfacial finite elements with tension-softening constitutive laws are inserted into the crack path to model energy dissipation in the fracture process zone, while the elastic bulk material is modelled by the SBFEM. The resultant nonlinear equation system is solved by local arc-length controlled solvers. A concrete beam subjected to mixed-mode fracture is modelled using the proposed method. The numerical results demonstrate that this new method can predict both satisfactory crack trajectories and accurate load-displacement relations with a small number of degrees of freedom.

1 INTRODUCTION

It is now generally accepted that the linear elastic fracture mechanics (LEFM) is only applicable to large-sized structures such as dams and not to normal-sized structures such as concrete beams, whereas the nonlinear fracture mechanics (NFM), considering the energy dissipation in the fracture process zone (FPZ), has wider applicability (Petersson 1981; Xie and Gerstle, 1995). Extensive literature reviews recently carried out by the authors (Yang and Proverbs, 2004; Yang and Chen, 2004; Yang and Chen, 2005; Yang, 2006) show that, although both the LEFM- and NFM-based finite element methods (FEM) have gained considerable success in modelling single-crack propagation problems, modelling multi-cracking is still in an infant stage. Even for single-cracked problems, the necessity of complex remeshing operations makes fully-automatic crack propagation modelling a cumbersome task (Wawrzynek and Ingraffea, 1989) in both LEFM- and NFM-based FEMs. Besides remeshing, two more difficulties are encountered in fully-automatic crack propagation modelling when the NFM-based methods are used. The first difficulty is the lack of a well-validated crack propagation criterion. The most intuitive criterion is the maximum principal stress (σ_1) criterion (e.g., Bocca et al, 1991; Carpinteri et al, 1993), which assumes the crack propagates perpendicular to the maximum principal stress direction when σ_1 at the crack tip reaches the material tensile strength. This criterion needs fine crack-tip meshes, such as a complex rosette used by Carpinteri et al (1993), to accurately calculate stresses at the crack tip, which exacerbates the complexity in remeshing. Wells and Sluys (2000) and Mariani S, Perego U (2003) also used this criterion within the framework of the extended finite element method (XFEM). The most distinct advantage of the XFEM in modelling crack propagation is that remeshing is completely avoided. However, a fine mesh must be used in the high stress-gradient regions to accurately calculate crack propagation direction. This infers that if the crack-path is unknown a priori, a very fine initial mesh is needed. The second difficulty is the need of a robust numerical solver to equation systems characterized with strong nonlinearity caused by a combination of factors such as material tensile softening, boundary changes and mesh changes. The latter two factors necessitate an accurate mesh mapping algorithm to transfer state variables (displacements and stresses) from the old mesh to the new mesh. The phenomenon of snapback further complicates the solution of nonlinear equation systems. Recent efforts (Yang and Proverbs, 2004; Yang and Chen, 2004) demonstrate that the so-called local arc-length methods (May and Duan, 1997) can effectively solve such complicated equation systems. However, this comes with high computational cost. In addition, numerical problems such as divergence and other errors of unknown origin may happen, especially for multiple crack propagation problems (Yang and Chen, 2005).

In order to avoid the above difficulties, a "semi-automatic" or two-step approach, i.e., the crack trajectories are automatically predicted by a LEFM-based method first, followed by a NFM-based modelling of the cracked structure, have been adopted, e.g., by Cendon et al (2000) and Galvez et al (2002). In these studies, the crack paths are predicted by the computer code FRAC2D, which uses a complicated remeshing procedure. The subsequent nonlinear problems are solved using ABAQUS by incorporating nonlinear springs or cohesive interface elements (CIEs) into special material subroutines. It should be noted that for such approach to be valid for normal-sized structures such as concrete beams, the crack paths predicted by the LEFM-based methods must be favourably compared with experimental observations. Fortunately, this seems to have been confirmed (e.g., Arrea and Ingraffea, 1983; Cendon et al, 2000; Galvez et al, 2002; Yang, 2006).

This study proposes a similar two-step approach to that of Galvez et al (2002). The difference is that this approach uses the recently-developed scaled boundary finite element (SBFEM) rather than the FEM. The SBFEM, developed recently by Wolf and Song (Wolf and Song, 1996; Wolf, 2003), is a semi-analytical method combining the advantages of the FEM and the boundary element method (BEM). It discretises domain boundaries only, so that the modelled spatial dimensions are reduced by one, as in the BEM, but it does not need fundamental solutions, as in the FEM. Therefore, the wide applicability of the FEM and the simplicity in remeshing of the BEM are retained. One significant advantage of the SBFEM is that stress singularities at cracks are analytically represented by the stress solutions so that accurate stress intensity factors (SIFs) can be calculated directly by definition. Consequently, fine crack-tip meshes or singular elements as required by the FEM are not needed. In addition, a domain may be divided into subdomains in any desired way and the density of nodes on the subdomain edges or domain boundaries can be specified according to the desired accuracy. This allows crack propagation to be modelled more flexibly than the FEM. These advantages of the SBFEM have been demonstrated recently by Yang (2006) in which a remeshing procedure as simple as used in the BEM was developed and successfully applied to a variety of mixed-mode crack propagation problems. The present study uses this simple remeshing procedure as the first step. CIEs are then inserted into the crack path, forming a finite element-SBFEM coupled nonlinear problem, which is solved by the local arc-length methods. Interested readers are referred to (Deeks and Wolf, 2002; Wolf 2003; Yang, 2006) for details of the SBFEM.

2 THE FIRST STEP: REMESHING BASED ON SBFEM AND LEFM

Fig. 1 illustrates the basic steps of the remeshing procedure (Yang, 2006) for the convenience of following discussion. Compared with remeshing procedures in the FEM (e.g., Wawrzynek and Ingraffea, 1989; Bocca et al, 1991), this remeshing procedure has the following advantages: (i) it is very simple because remeshing is carried on a few large-sized subdomains rather than many small finite elements, and in each remeshing step, only a few operations on edges and vertices of the subdomains are involved. Discretisation is conducted after remeshing by assigning nodal seeds to each edge and higher accuracy can be easily achieved by assigning edges with smaller nodal seeds; (ii) the degrees of freedom (DOFs) do not necessarily increase with remeshing because neither crack-tip mesh refinements nor singular elements are needed to calculate SIFs. And indeed for some cases, the DOFs may decrease with remeshing (Yang, 2006); and (iii) the SIFs calculated from the semi-analytical stress solutions are highly accurate, which ensures good predictions of crack trajectories even using a small number of DOFs. Interested readers can refer to (Yang, 2006) for a full description of the remeshing procedure.

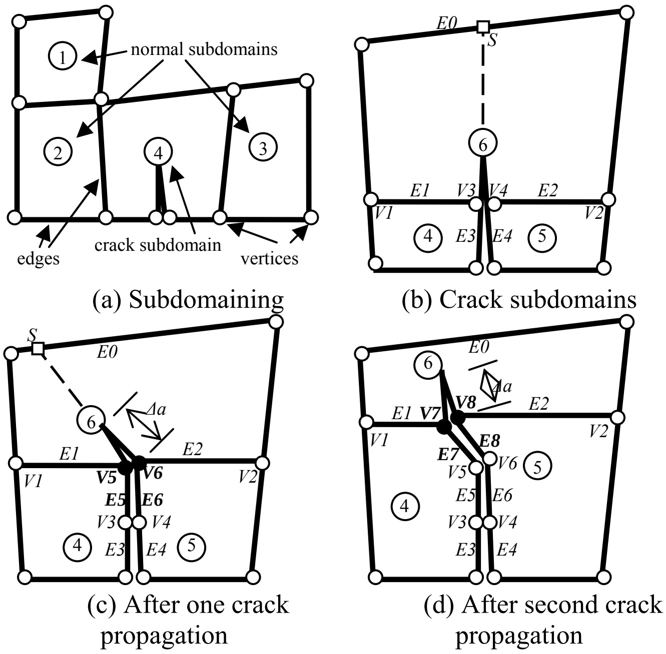

Figure 1. The first step: prediction of crack trajectory by a simple remeshing procedure based.

3 CONSTITUTIVE LAWS OF COHESIVE INTERFACE ELEMENTS

The crack is modelled by the fictitious crack model (Hillerborg et al, 1976) in the form of cohesive interface finite elements. Petersson's bi-linear σ-*COD* softening curve (Petersson, 1981) is used as the constitutive law of the CIEs in the normal direction, which is shown in Fig. 2a. A simple anti-symmetric τ–*CSD* relation as shown in Fig. 2b is assumed to model the shear resistance of the CIEs since there is little experimental data available in this respect. The loading-unloading paths are also indicated in Fig. 2. Both relations assume an "irreversible unloading path", i.e., when the crack closes, an elastic unloading occurs along the scant line as the *COD* or *CSD* decreases. The areas below the curves in Fig. 2a and Fig. 2b are the mode-I fracture energy G_f and the mode-II fracture energy G_{fII} respectively. The initial tensile stiffness k_{n0} before the concrete tensile strength f_t is reached should be high enough to represent the un-cracked material but not too high to cause numerical ill-conditioning. A reasonable initial shear stiffness k_{s0} is also needed before the ultimate shear stress τu is reached. If *COD* is negative during loading increments or iterations, a compressive stiffness of magnitude equal to the initial tensile stiffness k_{n0} is assigned to the CIEs in order to prevent penetration of crack surfaces. The four-noded interface elements developed by Xie and Gerstle (1995) are used to model the cohesive cracks.

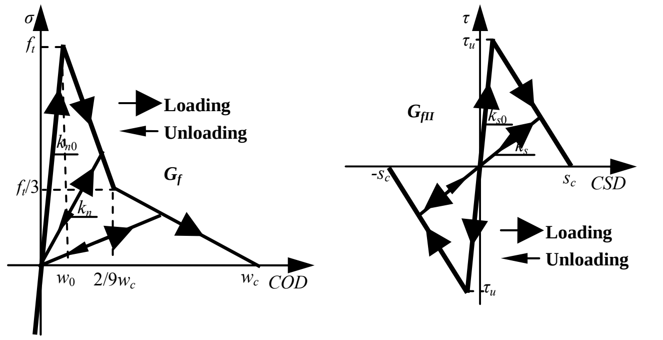

(a) normal traction σ-COD curve (b) shear stress τ-CSD curve

Figure 2. Constitutive laws of cohesive interface elements.

4 THE SECOND STEP: INSERTING COHESIVE INTERFACE ELEMENTS

Predicting the crack trajectory using the simple remeshing procedure (Figs 1a-d) based on the LEFM and the SBFEM is the first step of the proposed method. The second step is to insert the above-discussed CIEs into the predicted crack path (Fig. 1d) to model energy dissipation in the FPZ before a nonlinear analysis is carried out.

It should be noted that the two crack surfaces connected with the scaling centre of the crack subdomain S6 in Fig. 1d are not discretised, and thus the CIEs cannot be directly inserted to model these two surfaces. First, a new vertex (*V9*) is added at the scaling centre of the crack subdomain *S6* in Fig. 1d, forming two new edges (*E9* and *E10*) representing the crack surfaces connected with the crack-tip (Fig. 3a). The cracked subdomain *S6* is then subdivided into two subdomains (*S6* and *S7* in Fig. 3a) by adding a new edge *E11* and a new vertex *V10* which is the intersection point between the crack direction and the boundary edge *E0*. The edge *E0* is also divided into two edges *E0* and *E12*. The scaling centers of *S6* and *S7* can be conveniently placed at their geometrical centers. Second, all the edges which are not connected to any scaling center are discretised by assigning a global nodal seed (Fig. 3b). Because the edges *E9* and *E10* are not connected with any scaling centers anymore, they become normal edges and are also discretised. This allows the entire crack path to be inserted with CIEs, as shown in Fig. 3b, where the crack path is modeled by 8 CIEs.

The resultant problem is thus a nonlinear SBFEM-FEM coupled one. However, because the stiffness matrices and the equivalent nodal forces of the subdomains in the SBFEM and those of the CIEs are all based on the boundary nodes, they can be assembled to form the system stiffness matrix and equivalent nodal force vector without any difficulty. In fact, the assembling procedure is exactly the same as usually used in the FEM. The resultant nonlinear equation system is then solved by local arc-length method (Yang and Proverb, 2004; Yang and Chen, 2004).

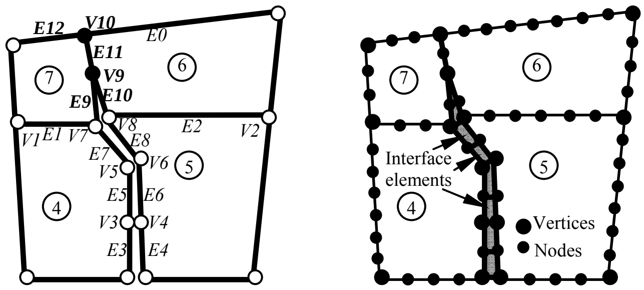

(a) Subdivision of the crack subdomain into two normal subdomains (b) Discretisation of edges and insertion of cohesive interface elements

Figure 3. The second step: inserting cohesive interface elements into the crack path.

5 NUMERICAL EXAMPLES, RESULTS AND DISCUSSION

The example is the four-point single-edge notched shear beam tested and analysed by Arrea and Ingraffea (1982). This shear beam has since become a benchmark to validate mixed-mode crack propagation modelling (Rots and De Borst, 1987; Xie and Gerstle, 1995; Cendon et al, 2000; Yang and Chen, 2004; Yang, 2006). The geometry and boundary conditions of Series B beams in the test are shown in Fig. 4. The available material properties from (Arrea and Ingraffea, 1982) are: E=24.8GPa and υ=0.18. The parameters defining the constitutive laws of CIEs are assumed as follows: G_f=100N/m, G_{fII}=0.1G_f=10N/m, f_t=3.0MPa,

$\tau_u=f_t/3=1.0$MPa, $w_0=0.0001$mm, $w_c=0.12$mm, $s_c=0.02$mm and $k_{n0}= k_{s0}=30000$MPa/mm.

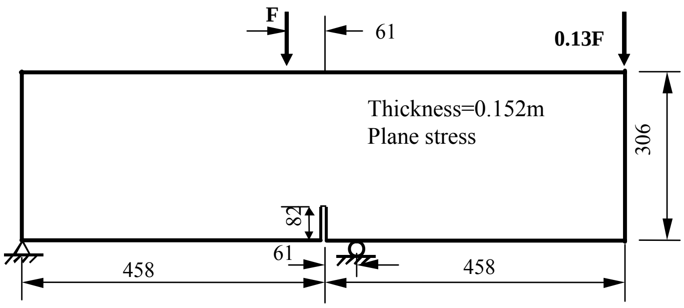

Figure 4. Four-point single edge-notched shear beam for mixed-mode crack propagation (unit: mm).

The beam is divided into 5 subdomains as shown in Fig. 5a. The scaling centres of S1 and S2 are positioned at the left-top corner and right-bottom corner respectively, so that their associated edges are not discretised. The initial number of nodes is 119 and most of them (81) are used to model S5 with the crack tip. Finer meshes are also modelled resulting in little difference in the displacement field. The elastic subdomains are modelled by 2-noded linear line elements. Eight Gaussian points are used in each CIE for the integration. In the first step, the smoothness of predicted crack trajectories is controlled by a constant incremental length Δa (ref. Fig. 1). A smaller Δa leads to a smoother crack trajectory. In solving the nonlinear equation systems, the global stiffness matrix is formed at the first iteration of every loading increment and remains unchanged during iterations afterwards, i.e., the modified Newton-Raphson iterative procedure is used.

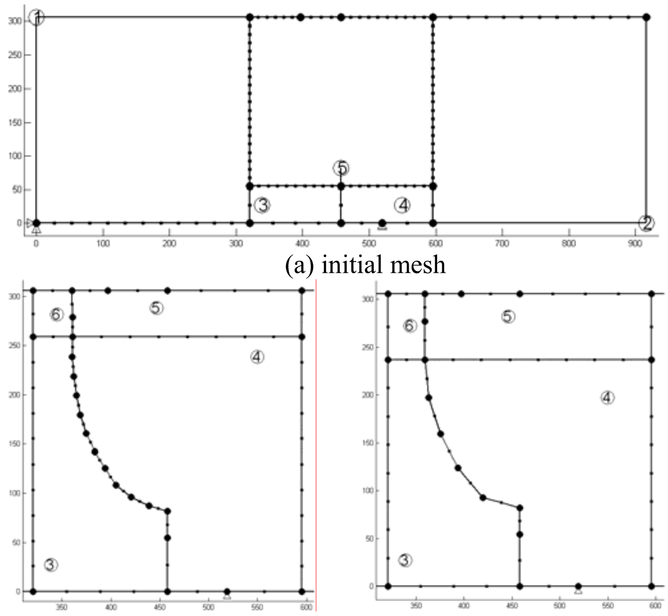

(a) initial mesh

(b) Δa=20mm (c) Δa=40mm

Figure 5. SBFEM meshes for the single notched shear beam.

Two crack increment lengths Δa=20mm and 40mm are used to predict the crack paths by the first step using the same initial mesh in Fig. 5a and the C_{max} criterion (Erdogan and Sih, 1963). There are 147 and 123 nodes in the final meshes for Δa=20mm and 40mm after 12 and 6 LEFM crack propagations respectively. Only slight increases in DOFs occur. The meshes in the core subdomains after the CIEs are inserted are shown in Fig. 5b and Fig. 5c respectively for the two crack increment lengths while the meshes outside the core subdomains are the same. One can see that using the same initial mesh, different crack increment lengths produce very consistent crack paths, which agree well with the experimental record.

Although the LEFM can predict satisfactory crack trajectories, it generally overestimates global structural responses considerably (Yang, 2006). Good structural responses can only be obtained when a NFM-based method is used, as demonstrated in Fig. 6 where the results from the present two-step method are compared favourably with the experimental data. This is due to the fact that only a NFM-based method can accurately model the FPZ which cannot be ignored in normal-sized concrete structures.

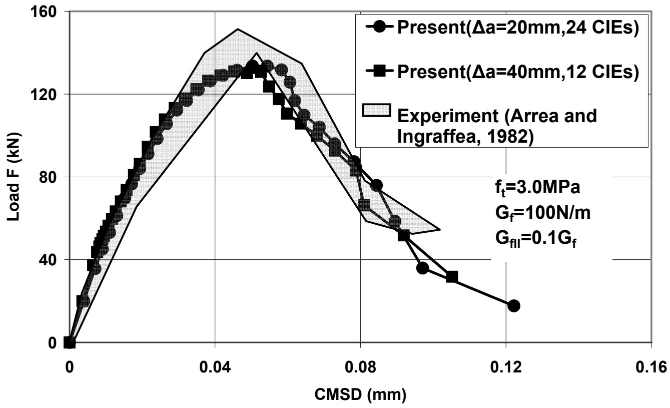

Figure 6. Load-CMSD predicted by the developed two-step method for the shear beam.

Figs 7-10 illustrate the evolution of the displaced configurations and the normal traction distributions along the crack path predicted by the two-step method. It can be seen that, at the peak load F=133.6kN (Fig. 7), the FPZ is slightly longer than $3\Delta a$=60mm and no real crack is formed. In the post-peak stage, the fictitious crack tip moves upwards as the crack opens. The real crack initiates at a load slightly higher than F= 87.4kN (Fig. 8b). At this load, the real crack tip predicted by the LEFM has already passed the midpoint of the beam after 7 crack propagations. As the load further drops, the FPZ rapidly shrinks from the lower end and the real crack extends upwards (Fig. 9b). Even at a very low load F=17.7kN the real crack extends only half of the beam depth (Fig. 10b) whereas the LEFM-based method has finished 12 crack propagations. The evolution of the normal traction profile from Δa=40mm is very close to Fig. 7-10, which indicates again that only a few long CIEs are sufficient to predict accurate results. This is also confirmed by Fig. 6 where slight discrepancy between the load-CMSD curves from these two crack increments exists only at the post-peak stage. This may save computational cost considerably when the modelled domain is large.

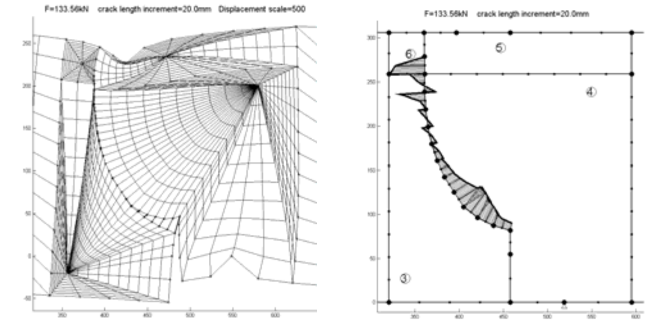

(a) displaced core subdomains (b) normal traction

Figure7. Displaced mesh and normal traction along the crack at F=133.6kN (peak load).

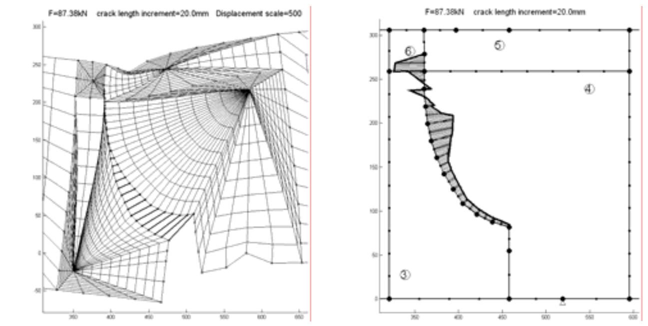

(a) displaced core subdomains (b) normal traction

Figure 8. Displaced mesh and normal traction along the crack at F=87.4kN.

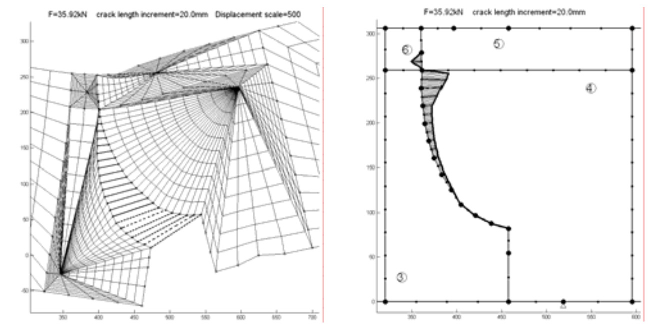

(a) displaced core subdomains (b) normal traction

Figure 9. Displaced mesh and normal traction along the crack at F=35.9kN.

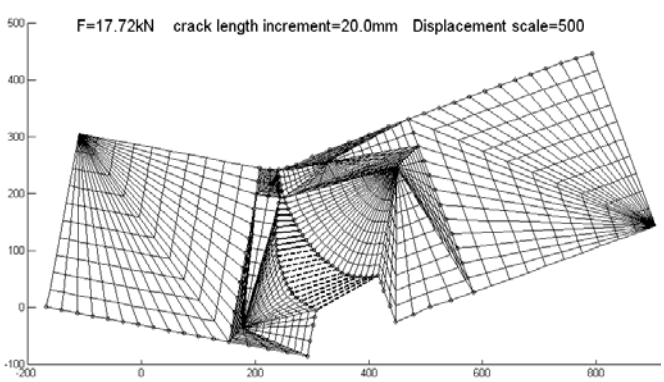

(a) displaced core subdomains

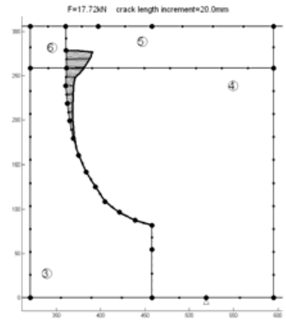

(b) normal traction

Figure 10. Displaced mesh and normal traction along the crack at F=17.7kN.

Fig. 11 shows the predicted load-loading point deflection using the two-step method. The strong snap-back phenomenon is well captured, which demonstrates the robustness of the adopted local arc-length method.

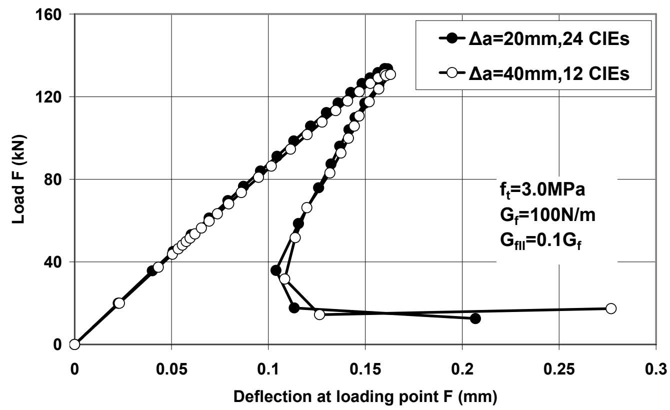

Figure 11. Predicted load-deflection at load point curves.

6 CONCLUSIONS

This study has developed a two-step SBFEM-FEM coupled method for semi-automatic modelling of cohesive crack propagation in quasi-brittle materials, in order to avoid various complexities involved in fully-automatic modelling approaches. The conclusions drawn from the numerical example are:

(a) the simple remeshing procedure based on SBFEM and the LEFM is able to predict satisfactory mixed-mode crack paths;

(b) due to the semi-analytical nature of SBFEM, a small number of DOFs allow accurate SIFs to be calculated. In addition, the increase in the number of DOFs during remeshing is kept to a minimum because of the flexibility in subdomaining and no special treatments such as refining crack-tip meshes or using singular element as needed in the FEM;

(c) the cohesive interface elements are effective in modelling energy dissipation in the FPZ and useful in analysing the evolution of the FPZ; and

(d) the local arc-length solver proves very powerful in tracing complex equilibrium paths characterised by strong snapback.

REFERENCES

Arrea M, Ingraffea AR (1982) Mixed-mode crack propagation in mortar and concrete. Report No. 81-13: Department of Structural Engineering, Cornell University

Bocca P, Carpinteri A, Valente S (1991) Mixed-mode fracture of concrete. International Journal of Solid Structures 27(9):1139-1153

Carpinteri A, Valente S, Ferrara G, Melchiorri G (1993) Is mode II fracture energy a real material property. Computers and Structures 48(3):397-413

Cendon DA, Galvez JC, Elices M, Planas J (2000) Modelling the fracture of concrete under mixed loading. International Journal of Fracture 103:293-310

Deeks AJ, Wolf JP (2002) A virtual work derivation of the scaled boundary finite-element method for elastostatics. Computational Mechanics 28(6):489–504

Erdogan F and Sih GC (1963). On the crack extension in plate under in plane loading and transverse shear, ASME Journal of Basic Engineering 85(4):519-527

Galvez JC, Cervenka J, Cendon DA, Saouma V (2002) A discrete crack approach to normal/shear cracking of concrete. Cement and Concrete Research 32:1567-1585

Hillerborg A, Modeer M, Petersson P (1976) Analysis of crack formation and crack growth in concrete by means of fracture mechanics and finite elements. Cement Concrete Research 6:773-782

Mariani S, Perego U (2003) Extended finite element method for quasi-brittle fracture. International Journal for Numerical Methods in Engineering 58:103-126

May IM, Duan Y (1997) A local arc-length procedure for strain softening. Computers and Structures 64(1-4):297-303

Moes N; Belytschko T (2002) Extended finite element method for cohesive crack growth. Engineering Fracture Mechanics 69(7):813-833

Petersson PE (1981) Crack growth and development of fracture zone in plain concrete and similar materials. Report TVBM-1006, Lund Inst. of tech., Lund, Sweden

Rots J, De Borst R (1987) Analysis of mixed-mode fracture in concrete. ASCE Journal of Engineering Mechanics 113(11):1739-1758

Wawrzynek PA, Ingraffea AR (1989) An interactive approach to local remeshing around a propagation crack. Finite Element in Analysis and Design 5:87-96

Wells GN, Sluys LJ (2000) Three-dimensional embedded discontinuity model for brittle fracture. International Journal of Solids and Structures 38(5):897-913

Wolf JP (2003) The scaled boundary finite element method. Chichester: John Wiley and Sons

Wolf JP, Song CM (1996) Finite-element modelling of unbounded media. Chichester: John Wiley and Sons

Xie M, Gerstle WH (1995) Energy-based cohesive crack propagation modelling. ASCE Journal of Engineering Mechanics 121(12):1349-1458

Yang ZJ (2006) Fully automatic modelling of mixed-mode crack propagation using scaled boundary finite element method. Engineering Fracture Mechanics 73(12):1711-1731

Yang ZJ, Chen JF (2005) Finite element modelling of multiple discrete cohesive crack propagation in reinforced concrete beams. Engineering Fracture Mechanics 72(14):2280-2297

Yang ZJ, Chen JF (2004) Fully automatic modelling of cohesive discrete crack propagation in concrete beams using local arc-length methods. International Journal of Solids and Structures 41(3-4):801-826

Yang ZJ, Proverbs D (2004) A comparative study of numerical solutions to nonlinear discrete crack modelling of concrete beams involving sharp snap-back. Engineering Fracture Mechanics 71(1):81-105